ISSN : 0974 - 7435 Volume 10 Issue 24

2014

BioTechnology

An Indian Journal

FULL PAPER

BTAIJ, 10(24), 2014 [15679-15686]

Stress and strain characteristics of rock and earth mass in a slope under the condition of underground mining

L.V.Yi-qing

College of mining engineering, Taiyuan University of technology, Taiyuan 030024, (CHINA)

ABSTRACT

As a typical example, Fengmaoding slope located in Gujiao, Taiyuan, was selected to analyze the stress and strain characteristics under the condition of underground mining, in mountain area. Geologic model was constructed based on the true data from Fengmaoding slope. Combined with the deformation mode of slope under the condition of exploit, numerical model was set up. And the stress and strain changes in the slope was simulated under the condition of underground mining. According to the simulation, failure deformation process was gotten. As a result, the main factors influencing the stability of the slope are the goaf underground and the faults in the slope.

KEYWORDS

Underground mining; Slope; Stress; Strain.

© Trade Science Inc.

INTRODUCTION

Researches about lithology of a slope are mainly descriptions of its physical characteristics, including soil texture and bedrock. The Fengmaoding slope studied in this paper is about 140m long and 210m wide. As a medium slope, it covers an area of 29400m, and its volume is 588000m. The direction of the principal axis is 318°, and the average grade is 50°[1]. The elevation of slope leading edge is 1036m, and that of the trailing edge is 1146m. It assumes the shape of an irregular semicircle on plan, and a convex shape in cross section. (Figure 1)

Based on field investigations, slope deformation and failure resulting from coal mining appear in the form of ground fissure and slope damage. We have discovered 25 fissures distributing on the top area (mainly) of Fengmaoding, as well as on the hillside and on both side of road and railway. The ground fissures, which are in a northeast to southwest direction and nearly parallel with the road and railway line, generally distribute in a linear fashion in the goaf area, and some of them distributes with branches, and parts of which extend in a wavy manner[2]. There are 7 ground fissures whose lengths of extension are 50～100m and 3 fissures whose lengths of extension are above 100m; the longest fissure is about 139m. They are mainly extensional fractures with different length and width, most of which are 2cm and the widest can be 15cm. Many fissures has been buried under slope wash[3].

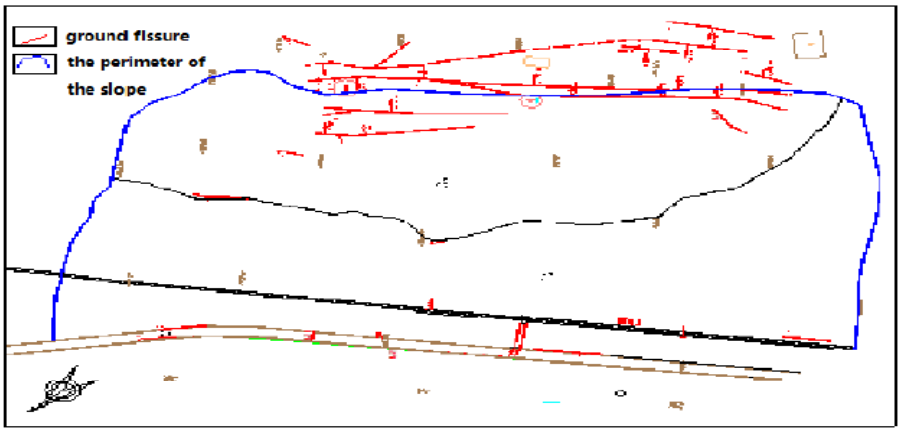

Figure1: Present situation of Fengmaoding slope

The large slope deformation is manifested as subsidence at the mountaintop, outward extrusion and dislocation at mountainside, and narrow compression ground fissures extending in a linear fashion and accompanied by ground uplift as well as the extrusion failure of buildings above the ground on both sides of the road at the foot of the mountain. Slope deformation and failure directly pose threats to the safety of the communication tower at the mountaintop, the railway and road at the bottom of the slope, as well as the village and river on the opposite side[4].

THREE-DIMENSIONAL NUMERICAL MODEL FOR THE SLOPE

Geological prototype

Based on field investigation and engineering geologic drilling, with the landform, topography, formation lithology, geologic structure and the engineering properties taken into consideration, we set up the generalized geological model of the Fengmaoding unstable slope engineering, as shown in Figure 2.

The finite element model

According to the actual landform of the slope, we build a model about 400m in width (X-direction) and about 470m in length (Y-direction). The lower boundary basement elevation is 850m; the upper boundary is up the earth's surface, and the maximum elevation is about 1170m[5].

Three problems needs to be considered in mesh generation. First, the geologic features of Fengmaoding slope and its underlying goaf need to be reflected. Elements in the location of fault, goaf and earth's surface, need subdivision to ensure that the geometric shapes of the rock mass are faithfully represented by the computational model[6]; second, the continuity of the calculation results of stress and displacement in numerical calculation need to be ensured; third, due to the limitations of the computing power and memory size of the computer, the element sizes need to be appropriate for the normal operation of the calculating program. According to the above principles, grids are divided and the 3D Finite element mesh computing model for Fengmaoding unstable slope is set up, as shown in Figure 3.

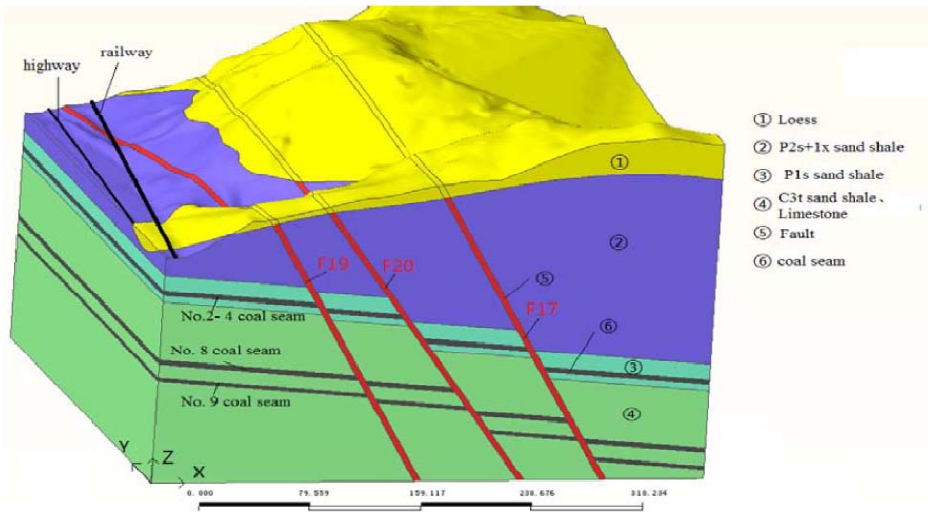

Figure 2: Engineering geology model of unstable slope at Fengmaoding

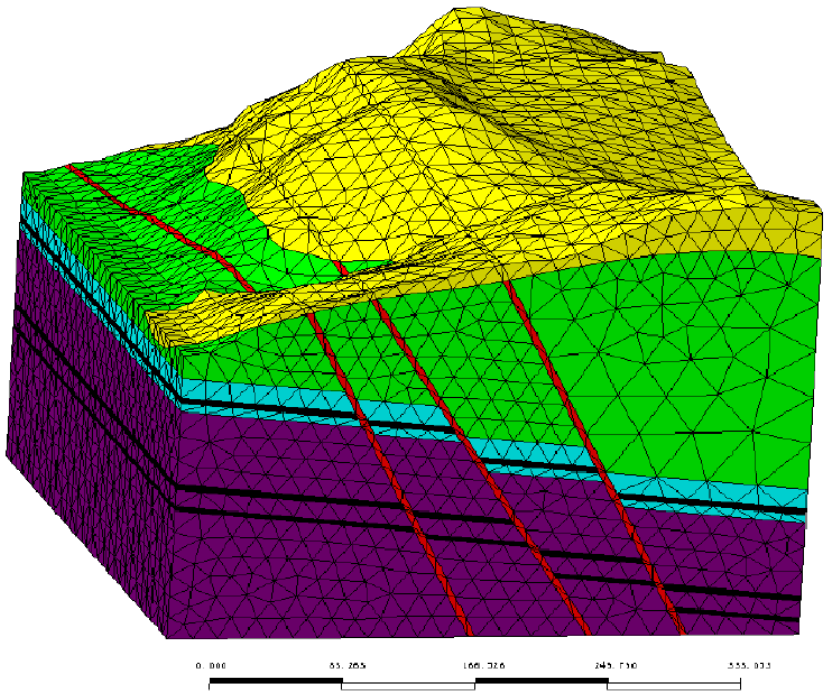

Figure 3: Mesh division of 3D finite element calculation model for unstable slope at Fengmaoding

Calculation condition and working condition

In the calculation model, the displacement constraint is used as the boundary condition, and constraints of X, Y and Z directions are used for all the node at the bottom. For boundary of Y-

direction, constraints of X-direction are chosen with Y and Z directions free; for boundary of X-direction, constraints of Y-direction are chosen with X and Z directions free. It means constraints are imposed on the left and right boundaries (X-direction), as well as the front and back boundaries (Y-direction) of the model, and the upper boundary are free boundary.

Only self-weight stress field is considered in the calculation, and all solid elements are adopted in the model[7]. We assume that the geotechnical materials are considered in terms of the elastoplasticity of homogeneous material, and their failures comply with the Mohr–Coulomb strength criterion[8]. At present, the commonly used rock mass plastic-yield criteria include M-C (Mohr-Cou1omb) criterion and the D-P (Drucker-Prager) criterion. Since the application of Mohr–Coulomb failure criterion in the numerical analysis of mass has been mature, and the relevant parameters in the model[9] can be calculated out from conventional tri-axial test, the Mohr-Coulomb model is adopted.

Based on exploration drilling information and rock mechanics laboratory test, and also referring to similar engineering experience, we choose the physical-mechanical parameters of rock and soil mass, as shown in TABLE 1.

The underground mining goafs on the coal seams of No.2 to No.4 under the Fengmaoding slope are studied in this paper. To reveal the nonlinear characteristics of surface deformation to underlying goaf, the following calculation and analysis of the working condition simulation are conducted.

(1) Base on the landform and topography, the formation lithology, and the geologic structure characteristics of the Fengmaoding unstable slope area, we make a balance calculation of the initial stress field, and clear the displacement values to zero. In this process, only the initial stress resulting from the self-weight of rock and soil mass is considered.

(2) Based on the goaf coverage determined according to field investigation, drilling and geophysical prospecting, we make an analysis about the response characteristics of the earth's surface deformation, displacement field, stress field and the plastic zone.

TABLE 1: Rock mass mechanics factors of Fengmaoding slope

Names of rock and soil mass	Volume weight γ (KN/m^3)		Shear strength				Elastic modulus E (Gpa)		Poisson's ratio μ
			Natural		Rainstorm				
	Natural	Rainstorm	c（Kpa）	φ（°）	c（Kpa）	φ（°）	Natural	Rainstorm	
Loess	17.40	18.70	33	22.40	18.00	20.20	0.20	0.16	0.45
Fault	18.00	19.00	30	30.00	27.60	27.60	0.40	0.37	0.43
P2s+1x sand shale	23.90	24.50	3500	46.10	3220.00	42.50	16.50	15.30	0.40
P1s sand shale	24.50	25.60	3520	46.80	3238.50	43.10	19.00	17.70	0.39
C3t sand shale、Limestone	25.70	26.30	3600	47.30	3312.00	43.50	19.50	18.30	0.38
coal seam	13.78	14.00	300	28.00	276.00	25.70	0.50	0.48	0.40
P2s+1x sand shale（regolith）	22.90	23.90	1800	28.50	90.00	21.00	8.20	7.20	0.43
P1s sand shale（regolith）	23.50	24.50	2020	30.00	261.00	23.00	10.00	8.50	0.41

THE ANALYSIS OF THE NUMERICAL SIMULATION RESULTS

The distribution of surface deformation

Figure 4 shows the whole displacement vector fields of the Fengmaoding unstable slope. It can be seen that, the directions of X-axis on the front of the slope at the foot of the mountain and the

footwall of the fault F20 (including the areas of railway and the road) are mainly negative, manifesting as displacement of outward extrusion to the free face and the outside deformation of the slope[10]. The X-axis directions of the hanging wall of fault F20 and the footwall of fault F17 are mainly positive, manifesting as the displacement of rock and soil mass towards the goaf due to coal seam mining and inward deformation of the slope. The displacement vector field in Y direction is complex, but mainly constrained by the subsidence of the massif to the goaf, manifesting as the displacement of the rock and soil mass on both sides above the goaf down to it. The displacement vector field in Z direction is relatively simple, mainly manifesting as subsidence. And due to coal seam mining, the downward displacement in Z-direction at the mountaintop is the largest. It is worth noting that the displacement field uplift in some local areas of the mountainsides above the railway corresponding to the actual displacement and deformation.

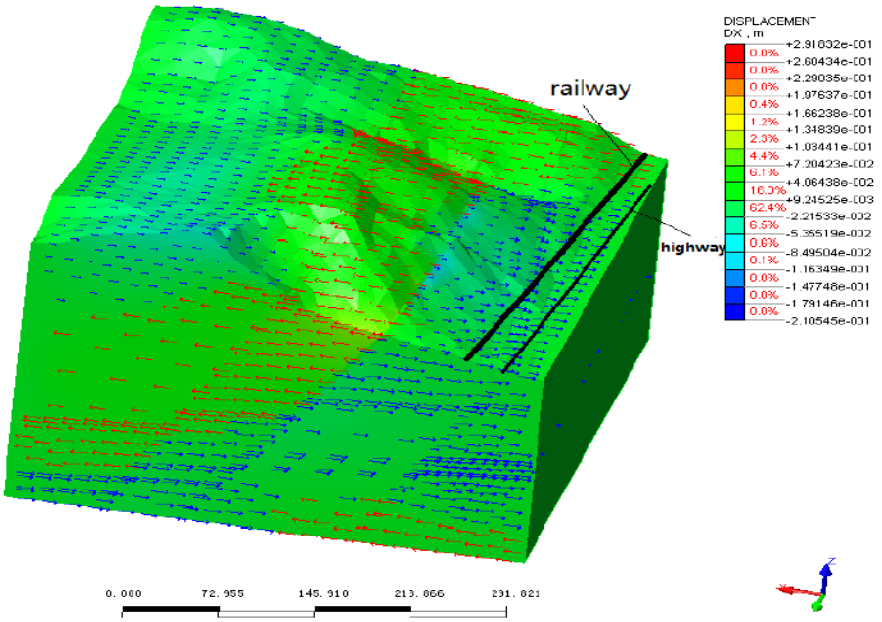

Figure 4: (a) Displacement vector field in X direction

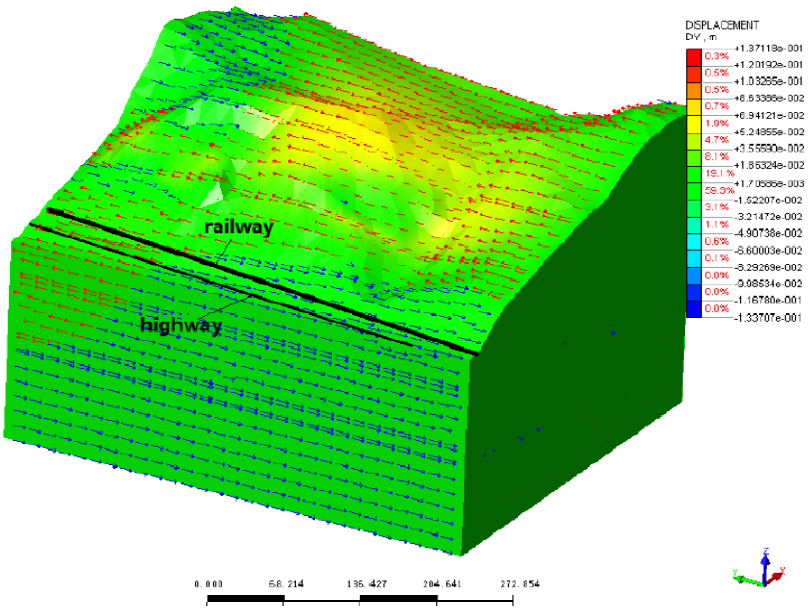

Figure 4: (b) Displacement vector field in Y direction

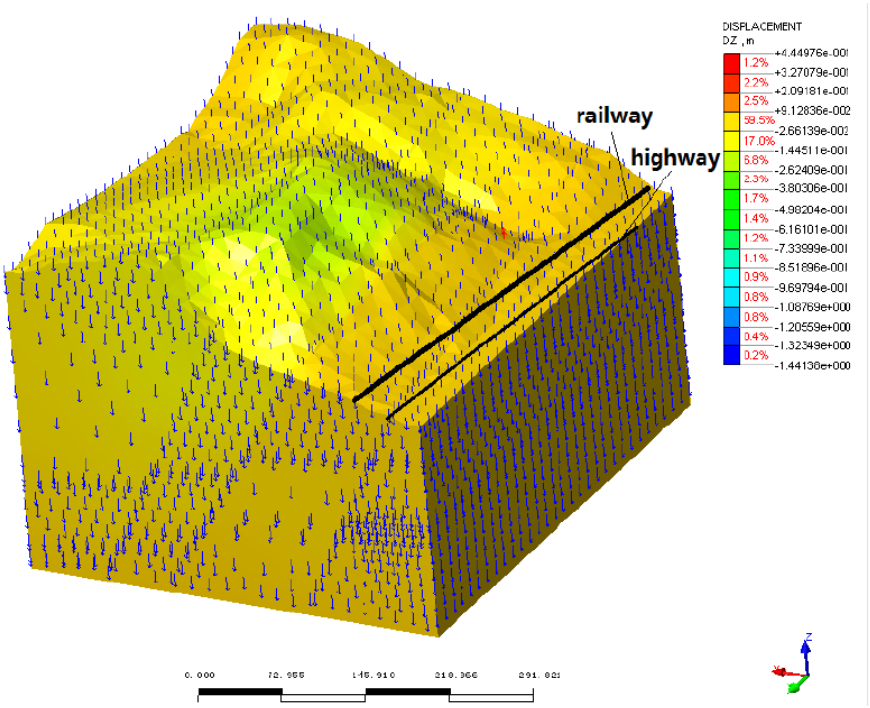

Figure 4: (c) Displacement vector field in Z direction

Feature analysis of the stress field

Figure 5 is the whole stress vector field of Fengmaoding unstable slope. The results of calculation show the direction of maximum principal stress is nearly parallel to the slope surface, and the minimum principal stress is perpendicular to the earth's surface, which mean the principal stress is controlled by the landform and topography of the earth's surface, and also influenced by faults where the stress concentration phenomenon occur. At the bottom of the model, the maximum principal stress is in vertical direction, and the minimum principal stress is in horizontal direction, indicating that the principal stress is controlled by the self-weight of rock and soil mass as well as the lateral pressure coefficient.

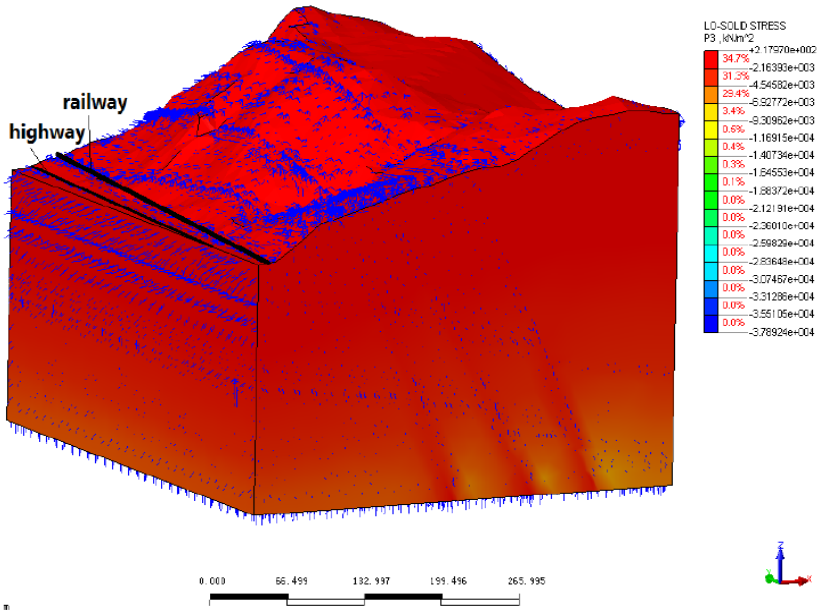

Figure 5: (a) The maximum principal stress and the vector graph

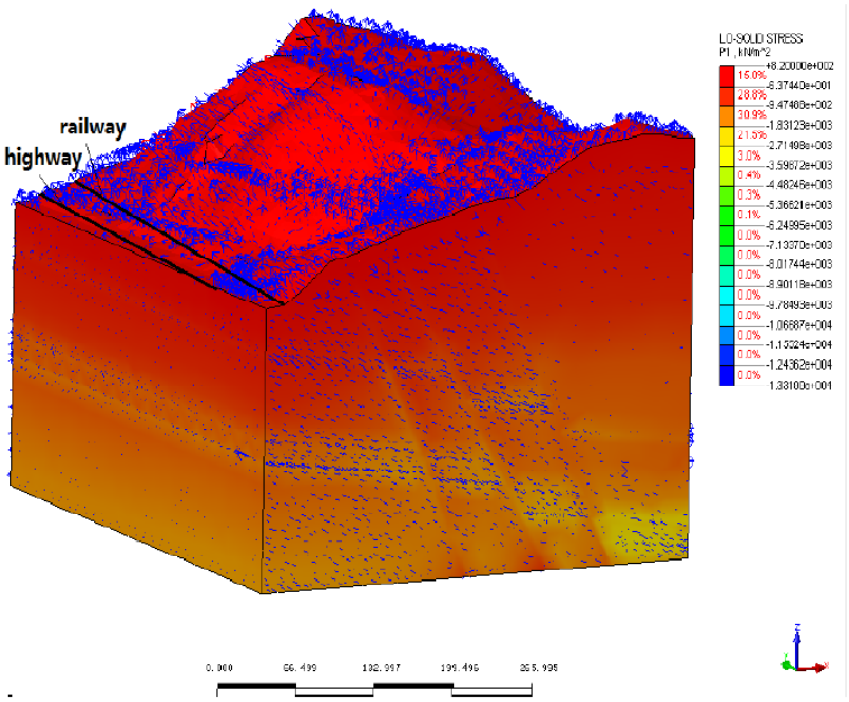

Figure 5: (b) The minimum principal stress and the vector graph

Feature analysis of the maximum shear strain

Figure 6 is the nephogram of the whole maximum shear strain of Fengmaoding unstable slope. It can be seen that the shear strain on the earth's surface, the mountaintop and the mountainside (close to the faults of F20 and F17) increases, and its magnitude is about 0.06. The shear failures of rock and soil mass in these areas are more likely to occur.

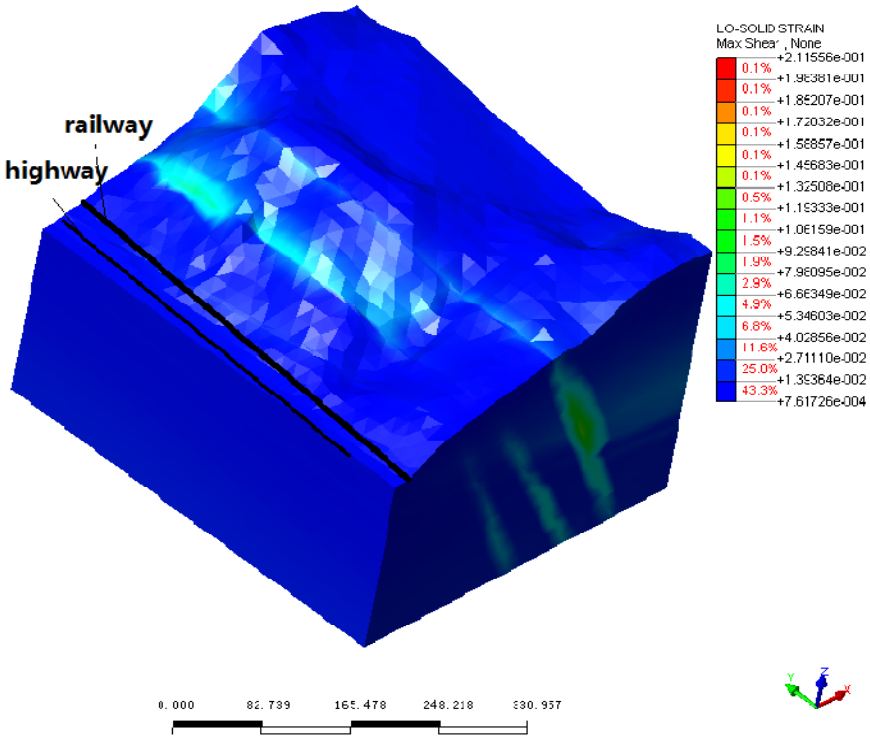

Figure 6: Whole cloud map of maximum shearing force

CONCLUSIONS

(1) Due to coal mining on NO.2～NO.4 seam, the stress field changes, and stress concentration occurred in the rock and soil mass near the goaf. For example, large stress concentration occurred in the upper part of the goaf on fault F20; tensile failure was likely to occur in the part connected with the goaf; compressive stress decreased in the lower part, indicating that the stress field of the rock and soil mass near the goaf was not only controlled by the self-weight stress field, but also heavily influenced by the goaf. The changes of stress field in fault F20 and part of fault F19 and F17 extended to the earth's surface; the minimum principal stress appeared as tensile stress, and tensile failure is likely to occur.

(2) The shear strain distribution of rock and soil mass was controlled by fault F20 and F17, as well as the goaf. In the south of the side slope, the maximum shear strain occurred near F17. In the northern and central part of the field, influenced by the goaf, the maximum shear strain was controlled by fault F20 and extends along F20 from the goaf to the earth's surface. While on the earth's surface, the maximum shear strain occurre near fault F20, and shear failure of the rock and soil mass was more likely to occur; then it was followed by fault F17, and the shear strain near F19 decreased.

(3) The goaf resulting from coal extraction would lead to the segment distributions of stress on the overlying strata above the goaf: the elastic zone and the plastic zone, and the stress peak area occurred in the junction area which was the interface between the stress increasing zone and stress decreasing zone of the overlying strata. This interface, which was a critical area of stress transfer after terrane breakup of the goaf, was the overlying strata of the unloading arch spring. The unloading arch was formed by the overlying strata above the goaf to bear the load which was then transferred to the terrane of arch spring. Based on these load transferring principles in mechanics, and also taking the existence of fault plane in the slope into account, we decomposed the oblique downward pressure of terrane (the transferred resultant force) into an up-sliding component force and a supporting component force. And the up-sliding component force promoted the up-movement of the broken blocks along the structural plane or the fault plane. Therefore, the phenomena of ground uplift and fissure, etc. occurred at the toe of the slope.

ACKNOWLEDGMENTS

This project is supported by the National Natural Science Foundation for Young Scholars of China (Grant No. 41103052)

REFERENCES

[1] H.Jan, B.Holger, H.B.Michael; The Implicit Power Motive and Sociosexuality in Men and Women: Pancultural Effects of Responsibility, Journal of Personality and Social Psychology, **99(2)**, 380 –394 **(2010)**.

[2] David De Cremer, Eric Van Dijk; When and why leaders put themselves first: leader behaviour in resource allocations as a function of feeling entitled, European Journal of Social Psychology, **35(4)**, 553–563 **(2005)**.

[3] A.D.Galinsky, D.H.Gruenfeld, J.C.Magee; From power to action, Journal of Personality and Social Psychology, **85(3)**, 453–466 **(2003)**.

[4] C.J.Torelli, S.Shavitt; Culture and concepts of power, Journal of Personality and Social Psychology, **99(4)**, 703–723 **(2010)**.

[5] C.Zhong, J.C.Magee, W.W.Maddux, A.D.Galinsky; Power,culture, and action: considerations in the expression and enactment of power in east asian and western societies, In E.A.Mannix, M.A.Neale, & Y.Chen (Eds.), Research on Managing in Teams and Groups, **9**, 53–73 **(2006)**.

[6] Y.Trope, N.Liberman; Construal-Level Theory of Psychological Distance, Psychological Review, **117**, 440–463 **(2010)**.

[7] Pamela K.Smith, Danie, H.J.Wigboldus , A.P.Dijksterhuis; Abstract thinking increases one's sense of power, Journal of Experimental Social Psychology, **44**, 378–385 **(2008)**.

[8] L.Joris, A.S.Diederik; How Power Influences Moral Thinking, Journal of Personality and Social Psychology, **97(2)**, 279 –289 **(2009)**.

[9] A.L.Freitas, P.M.Gollwitzer, Y.Trope; The influence of abstract and concrete mindsets on anticipating and guiding others' self-regulatory efforts, Journal of Experimental Social Psychology, **40**, 739–752 **(2004)**.

[10] Nathanael J.Fast, Nir Halevy, Adam D.Galinsky; The destructive nature of power without status, Journal of Experimental Social Psychology, **48(1)**, 391–394 **(2012)**.